Electronic Supplementary Information

A Hepatocyte-Targeting Near-infrared Ratiometric Fluorescence Probe for Mornitoring Peroxynitrite during Drug-Induced Hepatotoxicity and its Remediation

Wen-Li Jiang,[a] Yongfei Li,[a,b] Wen-Xin Wang,[a] Yi-Ting Zhao,[a] Junjie Fei,[a] and Chun-Yan Li*[a]

[a] Key Laboratory for Green Organic Synthesis and Application of Hunan Province, Key Laboratory of Environmentally Friendly Chemistry and Applications of Ministry of Education, College of Chemistry, Xiangtan University, Xiangtan, 411105, PR China.

[b] College of Chemical Engineering, Xiangtan University, Xiangtan, 411105, PR China.

*Corresponding Author. E-mail: lichunyan79@sina.com.

Table of contents

1. Experimental Section.

Reagents and apparatus. 9-Formyl-8-hydroxyjulolidine, ethyl acetoacetate, piperidine, 2-(4-diethylamino-2-hydroxybenzoyl) benzoicacid, N-(3-dimethylaminopropyl)-N'-ethylcarbodiimide hydrochloride (EDC·HCl), N,N-dimethylpyridin-4-amine (DMAP), 2,3,4,6-tetra-O-acetyl-α-D -galactopyranosyl bromide, sodium azide, sodium ascorbate, sodium methoxide, 4-acetamidophenol (APAP) were purchased from Aladdin (Shanghai, China). 3-Morpholinosydnonimine hydrochloride (SIN-1), minocycline hydrochloride, lipopolysaccharide (LPS), glutathione (GSH), N-acetylcysteine (NAC), biphenyldicarboxylate (DDB), cysteine (Cys) were purchased from Sigma-Aldrich (St. Louis, USA). Unless noted, all the chemicals were of analytical reagent grade and used as received without further purification.

Nuclear magnetic resonance (NMR) spectra were measured on a Bruker Avance II NMR spectrometer (Germany). ^{1}H NMR and ^{13}C NMR were conducted at 400, 100 MHz, respectively. Mass spectra (MS) was recorded on a Bruker Autoflex MALDI-TOF mass spectrometer (Germany). Element analysis was operated on Perkin Elmer 2400 elemental analyzer (USA). The fluorescence spectra were obtained on a Hitachi F-4600 spectrophotometer (Japan). The absorption spectra were collected on an Agilent CARY 60 UV-vis spectrophotometer (USA). HPLC was carried out on an Agilent 1260 LC system with a C18 column (USA). Fluorescence imaging of cells was carried out by an Olympus FV1000 laser confocal microscope (Japan). Fluorescence imaging of mice was performed on an IVIS Lumina XR small animal optical in vivo imaging system (USA).

General procedure for fluorescence measurement. The stock solution of Gal-NIR (500

μM) was prepared by dissolving Gal-NIR in MeOH. The stock solution of $ONOO^-$ was prepared by mixing three solutions, including hydrogen peroxide (0.7 M), hydrochloric acid (0.6 M), sodium nitrite (0.6 M) and sodium hydroxide (1.5 M). The concentration of the $ONOO^-$ stock solution was calculated by measuring the absorbance at 302 nm with a molar extinction coefficient of 1670 $M^{-1}cm^{-1}$. The solution of Gal-NIR with $ONOO^-$ was prepared with 50 μL Gal-NIR stock solution and appropriate volume of $ONOO^-$ stock solution, and then were diluted to 5 mL with phosphate buffer solution (PBS, 20 mM, pH 7.4). The fluorescence spectra were recorded with the excitation at 440 nm and the emission was collected at 450-820 nm. The excitation slit and emission slit were both set at 5.0 nm.

Cell incubation and fluorescence imaging. HepG2 (human hepatoma cells), HCT116 (human colon cancer), Hela (human cervix cancer) and MCF-7 (human breast cancer cells) were obtained from the State Key Laboratory of Chemo/Biosensing and Chemometrics of Hunan University (Changsha, China). The cells were cultured in DMEM (Dulbecco's modified Eagle's medium) supplemented with 10 % FBS (fetal bovine serum) and 1% antibiotics (100 U/mL penicillin and 100 μg/mL streptomycin) at 37 °C in a 5% CO_2 atmosphere.

The hepatocyte-specific experiments in four kinds of cells. The cells were divided into two groups. The first group was incubated with Gal-NIR (5 μM) for 30 min. The second group was incubated with NIR (5 μM) for 30 min.

Exogenous and endogenous $ONOO^-$ imaging experiments in HepG2 cells. The cells were divided into four groups. The first group was incubated with Gal-NIR (5 μM) for 30 min. The second group was incubated with SIN-1 (100 μM) for 30 min and then treated with Gal-NIR (5.0 μM) for 30 min. The third group was pretreated with LPS (1 mg/mL) for 10 h and then

incubated with Gal-NIR (5 μM) for 30 min. The fourth group was pretreated with Cys (200 μM) for 30 min, followed by treating with LPS (1 mg/mL) for 10 h and then stained with Gal-NIR (5 μM) for 30 min.

APAP-induced hepatotoxicity and its remediation in HepG2 cells. The cells were divided into five groups. The first group was incubated with Gal-NIR (5.0 μM) for 30 min. The second group was pretreated with APAP (500 μM) for 12 h and then incubated with Gal-NIR (5 μM) for 30 min. In the third to fifth group, the cells were pretreated with GSH (400 μM), NAC (400 μM), DDB (400 μM) for 1 h, followed by incubating with APAP (500 μM) for 12 h, and then treated with Gal-NIR (5 μM) for 30 min.

All the cells were washed by PBS buffer solution three times before fluorescence image and all images were obtained by confocal fluorescence microscope.

Fluorescence imaging in mice. BALB/c mice were purchased from Hunan SJA Laboratory Animal Co., Ltd (Changsha, China), used and kindly kept in all the experimental process. All animal operation was carried out according to the regulations issued by the Ethical Committee of Xiangtan University.

The hepatocyte-specific experiments. The mice was divided into two groups. The first group received an intravenous injection of NIR (100 μL, 200 μM). The second group was given an intravenous injection of Gal-NIR (100 μL, 200 μM).

APAP-induced hepatotoxicity and its remediation. The mice was divided into four groups. The first group received an intraperitoneal injection of APAP (500 mg/kg) and intravenous injection of Gal-NIR (100 μL, 200 μM). The second to fourth group were given an intravenous injection of 400 mg kg^{-1} GSH, 400 mg kg^{-1} NAC, 400 mg kg^{-1} DDB, respectively. 1 h later, the

mice were injected intraperitoneally with 500 mg kg^{-1} APAP. And the three group mice were then injected intravenously with Gal-NIR (100 μL, 200 μM).

All the mice were placed into the imaging chamber and imaged by small animal optical in vivo imaging system.

Histology analysis was carried out by sacrificing the mice after the above treatments. The livers were fixed in 4% paraformaldehyde solution, and then embedded in paraffin. The sliced liver tissues were stained with hematoxylin and eosin (H&E) and then observed by an optical microscope.

2. Synthesis of probes.

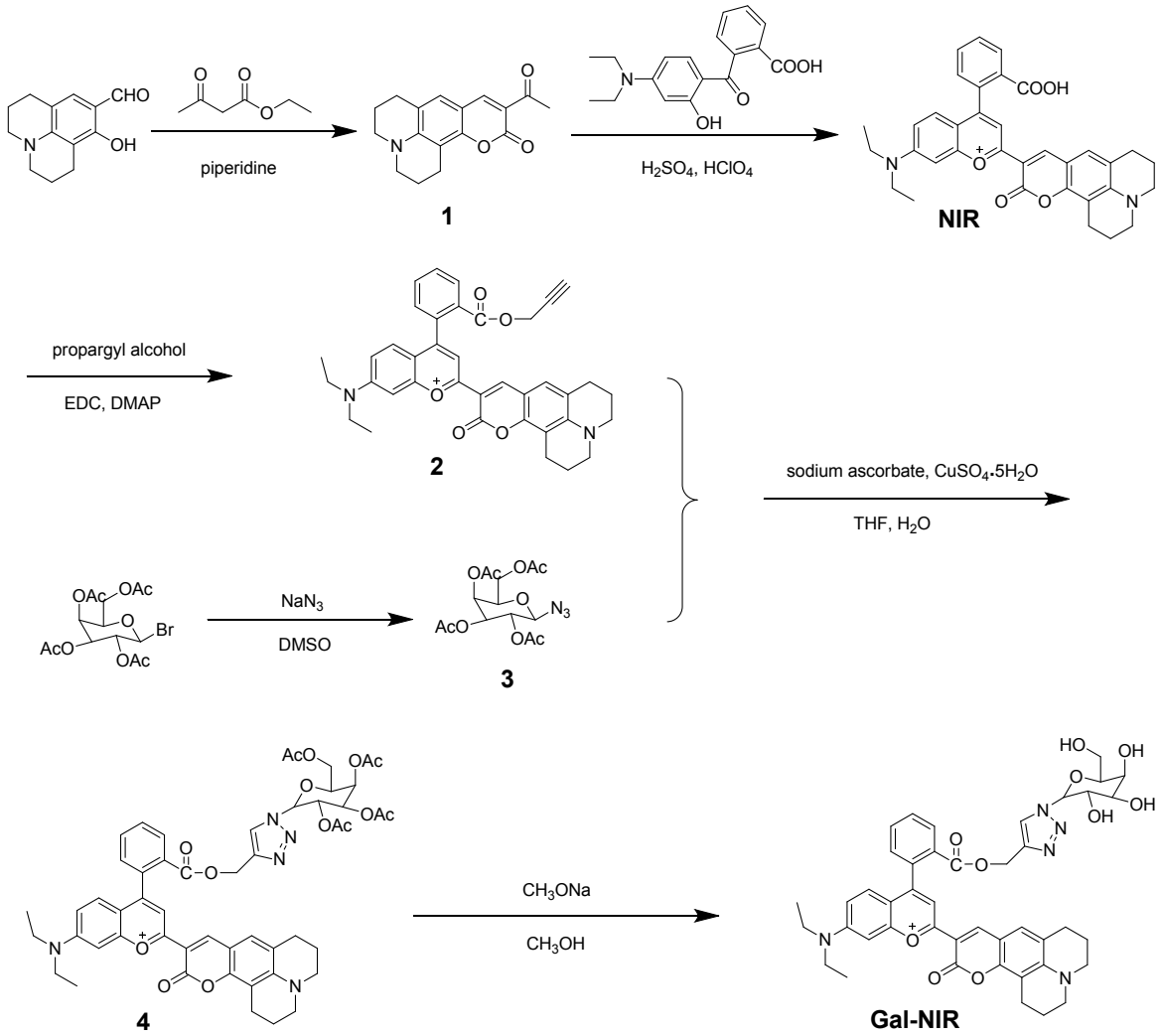

Scheme S1. Synthetic route for Gal-NIR.

Compound 1. 9-Formyl-8-hydroxyjulolidine (1.09 g, 5 mmol), ethyl acetoacetate (0.63 mL, 5 mmol), and piperidine (0.035 mL, 0.5 mmol) were dissolved in anhydrous ethanol (20 mL). After stirring and refluxing for 6 h, the reaction mixture was cooled and the solvent was evaporated. The residue was subjected to silica gel chromatography with CH_2Cl_2 as eluent to afford a deep yellow solid product. Yield: 0.85 g (60%). ^{1}H NMR (400 MHz, $CDCl_3$, ppm) δ 8.33 (s, 1H), 6.96 (s, 1H), 3.36 (t, J = 8.0 Hz, 4H), 2.87 (t, J = 8.0 Hz, 2H), 2.75 (t, J = 8.0 Hz, 2H), 2.66 (s, 3H), 1.97 (t, J = 8.0 Hz, 4H), MS (TOF): 284.1.

Compound NIR. Compound 1 (0.42 g, 1.48 mmol) and 2-(4-diethylamino-2-hydroxybenzoyl) benzoicacid (0.46 g, 1.48 mmol) were dissolved in H_2SO_4 (8 mL). The mixture was stirred at 90 °C for 12 h. After cooled to room temperature, the solution was poured into ice water and 70% perchloric acid (0.8 mL) was added to precipitate the solid. After filtered, the solid was dissolved in DCM (20 mL), washed with water and dried over anhydrous Na_2SO_4. The residue was then subjected to silica gel chromatography with CH_2Cl_2/CH_3CH_2OH (20/1, v/v) as eluent to obtain a green solid product. Yield: 0.39 g (40%). ^{1}H NMR (400 MHz, DMSO-d_6, ppm) δ 8.85 (s, 1H), 8.11 (d, *J* = 8.0 Hz, 1H), 7.82 (t, *J* = 8.0 Hz, 1H), 7.74 (t, *J* = 8.0 Hz,1H), 7.48 (d, *J* = 8.0 Hz, 1H), 7.27 (s, 1H), 7.14 -7.05 (m, 4H), 3.58 (d, *J* = 8.0 Hz, 4H), 3.43 (s, 4H), 2.72 (d, *J* = 4.0 Hz, 4H), 1.88 (s, 4H), 1.20 (t, *J* = 8.0 Hz, 6H). ^{13}C NMR (100 MHz, DMSO-d_6, ppm) δ 167.1, 159.9, 158.3, 157.2, 154.0, 152.5, 150.7, 144.3, 144.2, 133.0, 130.4, 130.2, 130.1, 129.1, 128.3, 125.1, 121.4, 109.7, 105.4, 96.1, 50.4, 49.8, 45.1, 26.7, 20.3, 19.3, 12.5. MS (TOF): 561.2.

Compound 2. Compound NIR (0.36 g, 0.55 mmol), propargyl alcohol (0.032 mL, 0.55 mmol), EDC·HCl (0.11 g, 0.55 mmol) and DMAP (0.013 g, 0.11 mmol) were combined in a Schlenk tube. Dry DCM (5 mL) was injected and the reaction tube was wrapped with Al foil. The reaction mixture was stirred at room temperature under N_2 atmosphere for 4 h. The reaction mixture was added with DCM and washed with 0.1 M HCl (20 mL), 20 mL of brine. The organic phase was collected and dried by using anhydrous Na_2SO_4. The solvent was evaporated under reduced pressure and the crude product was subjected to silica gel chromatography with CH_2Cl_2/MeOH (50/1, v/v) as the eluent to give a green solid product. Yield: 0.24 g (62%). ^{1}H NMR (400 MHz, $CDCl_3$, ppm) δ 9.34(s, 1H), 8.26 (d, *J* = 7.6 Hz, 1H), 7.80 (t, *J* = 8.0 Hz, 1H),

7.72 (t, J = 7.6 Hz, 1H), 7.65 (s, 1H), 7.44 (d, J = 7.2 Hz, 2H), 7.16 (d, J = 8.0 Hz, 2H), 6.93 (d, J = 8.0 Hz, 1H), 4.67 (d, J = 2.4 Hz, 2H), 3.71 (d, J = 5.6 Hz, 4H), 3.48 (t, J = 5.6 Hz, 5H), 2.93-2.85 (m, 4H), 2.03 (s, 4H), 1.39 (t, J = 8.0 Hz, 6H). MS (TOF): 599.6.

Compound 3. 2,3,4,6-Tetra-O-acetyl-α-D-galactopyranosyl bromide (0.82 g, 2.0 mmol) and sodium azide (0.65 g, 10 mmol) were dissolved in dry DMSO (3 mL). After stirring at room temperature for 30 min, the reaction mixture was then diluted with water (20 mL) and extracted with ethyl acetate (50 mL). The organic layer was then dried with anhydrous sodium sulfate and the solvent was removed by evaporation under reduced pressure. The residue was subjected to silica gel chromatography with ethyl acetate/petroleum ether (1/2, v/v) as the eluent to give a white solid product. Yield: 0.72 g (91%). ^{1}H NMR (400 MHz, $CDCl_3$, ppm) δ 5.44 (d, J = 3.2 Hz, 1H), 5.20-5.15 (m, 1H), 5.06 (dd, J = 3.6, 3.6 Hz, 1H), 4.63 (d, J = 8.8 Hz, 1H), 4.19-4.16 (m, 2H), 4.05 (t, J = 7.2 Hz, 1H), 2.19 (s, 3H), 2.11 (s, 3H), 2.08 (s, 3H), 2.00 (s, 3H); MS (TOF): 396.1.

Compound 4. Compound **2** (0.24 g, 0.35 mmol), compound **3** (0.28 g, 0.70 mmol), sodium ascorbate (0.006 g, 0.03 mmol) and $CuSO_4 \cdot 5H_2O$ (0.004 g, 0.015 mmol) were added in a solution of THF and water (5 mL/2 mL). Under N_2 atmosphere, the mixture was stirred at room temperature for 12 h. After the materials were consumed completely, the reaction mixture was washed three times with water and extracted with dichloromethane. The organic phase was dried over anhydrous Na_2SO_4. The solvent was evaporated, and the residue was purified by silica column chromatography using CH_2Cl_2/MeOH (10/1, v/v) as the eluent to give a green solid product. Yield: 0.082 g (22%). ^{1}H NMR (400 MHz, $CDCl_3$, ppm) δ 9.29 (s, 1H), 8.27 (d, J = 8.0 Hz, 1H), 7.88 (s, 1H),7.76 (t, J = 8.0 Hz, 1H), 7.68 (t, J = 8.0 Hz, 1H), 7.53 (s, 1H), 7.40

(d, J = 8.0 Hz, 1H), 7.16 (d, J = 8.0 Hz, 2H), 6.96 (d, J = 8.0 Hz, 2H), 5.60 (d, J = 8.0 Hz, 1H), 5.35 (s, 2H), 5.19-5.09 (m, 4H), 4.12 (d, J = 8.0 Hz, 2H), 3.73 (d, J = 8.0 Hz, 4H), 3.50 (s, 4H), 2.89 (d, J = 8.0 Hz, 4H), 2.18 (m, 12H), 2.03 (d, J = 8.0 Hz, 4H), 1.37 (t, J = 8.0 Hz, 6H). MS (TOF): 972.2.

Compound Gal-NIR. Compound **4** (0.082 g, 0.077 mmol) in dry MeOH (8 mL) was added in sodium methoxide (0.05 g, 0.92 mmol). After stirring for 24 h at room temperature, the mixture was neutralized by addition of HCl (1.0 M) until pH 7. The solvent was removed by evaporation under vacuum and the crude product was purified by silica column chromatography using CH_2Cl_2/MeOH (4/1, v/v) as the eluent to give a green solid product. Yield: 0.022 g (31%). ^{1}H NMR (400 MHz, DMSO-d_6, ppm) δ 8.28 (s, 1H), 8.15 (d, J = 8.0 Hz, 1H), 8.09 (s, 1H), 7.86 (t, J = 8.0 Hz, 1H), 7.77 (t, J = 8.0 Hz, 1H), 7.52 (d, J = 8.0 Hz, 1H), 7.16 (d, J = 8.0 Hz, 2H), 7.06 (d, J = 8.0 Hz, 2H), 7.01 (s, 1H), 5.43 (d, J = 8.0 Hz, 1H), 5.29 (s, 2H), 4.21 (d, J = 8.0 Hz, 2H), 4.11 (d, J = 8.0 Hz, 1H), 4.01 (d, J = 8.0 Hz, 1H), 3.80 (d, J = 16.0 Hz, 1H), 3.70 (d, J = 8.0 Hz, 1H), 3.62 (d, J = 4.0 Hz, 4H), 3.47 (s, 4H), 3.13 (d, J = 8.0 Hz, 4H), 2.77 (d, J = 8.0 Hz, 4H), 1.90 (s, 4H), 1.23 (t, J = 8.0 Hz, 6H); ^{13}C NMR (100 MHz, DMSO-d_6, ppm): δ 167.5, 165.3, 160.0, 158.8, 158.1, 155.1, 153.2, 153.1, 151.5, 149.3, 148.4, 140.8, 140.6, 136.4, 133.8, 132.4, 132.1, 130.1, 129.1, 123.8, 122.0, 115.4, 111.5, 110.5, 110.4, 96.9, 88.6, 79.1, 70.2, 69.9, 61.0, 58.5, 50.9, 50.3, 49.0, 45.8, 45.7, 27.0, 23.7, 22.8, 22.5, 11.3; MS (TOF): 804.3. Elem. anal. (%) calcd. for $C_{44}H_{46}ClN_5O_{14}$: C, 58.44, H, 5.13, N, 7.74. Found: C, 58.43, H, 5.14, N, 7.72.

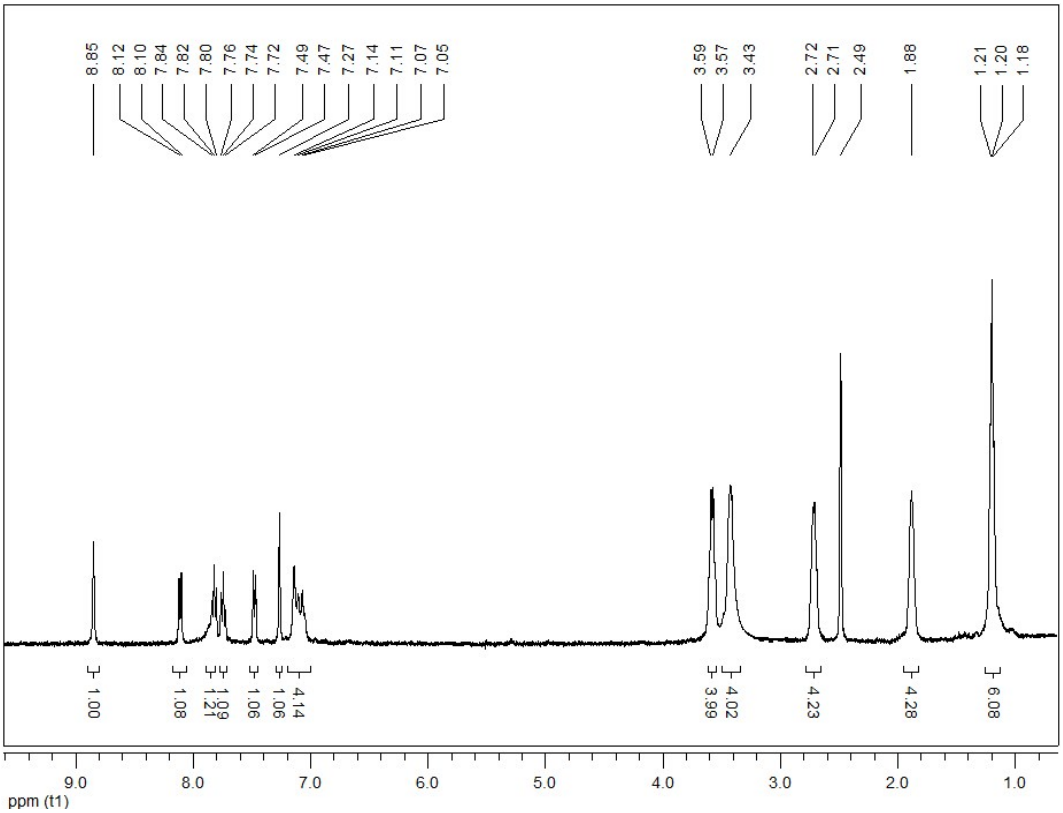

Fig. S1. ^{1}H NMR spectra of compound NIR in DMSO-d_6

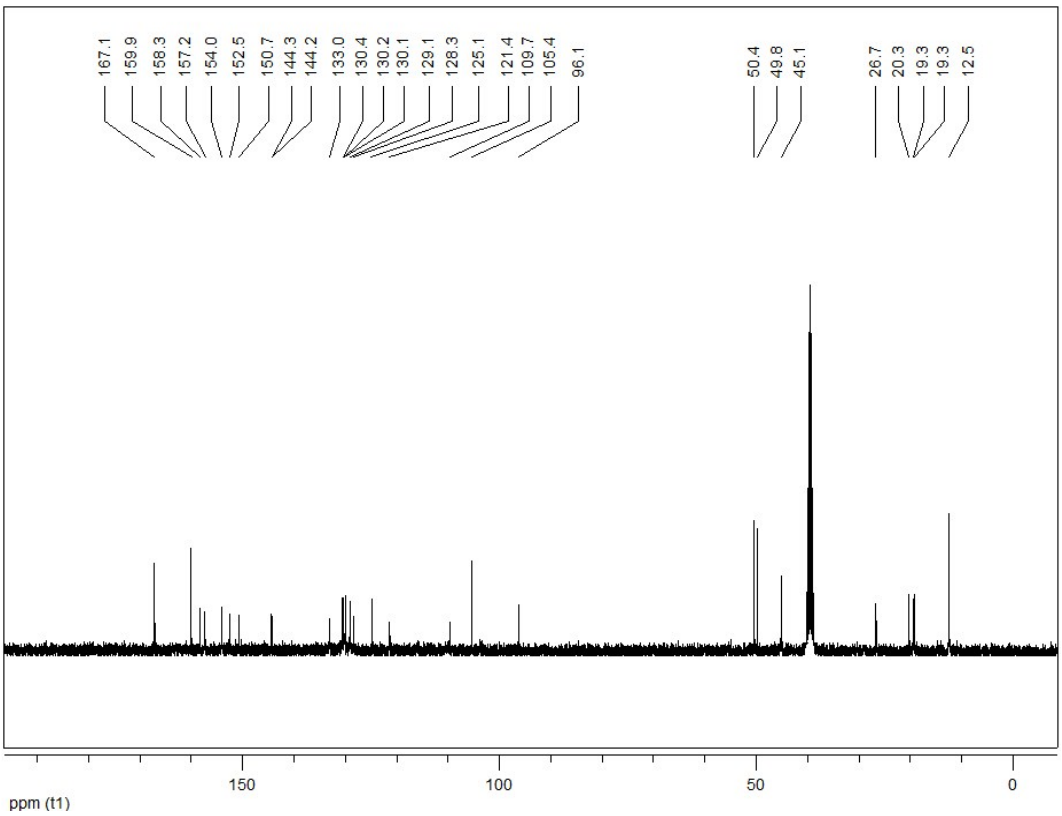

Fig. S2. ^{13}C NMR spectra of compound NIR in DMSO-d_6.

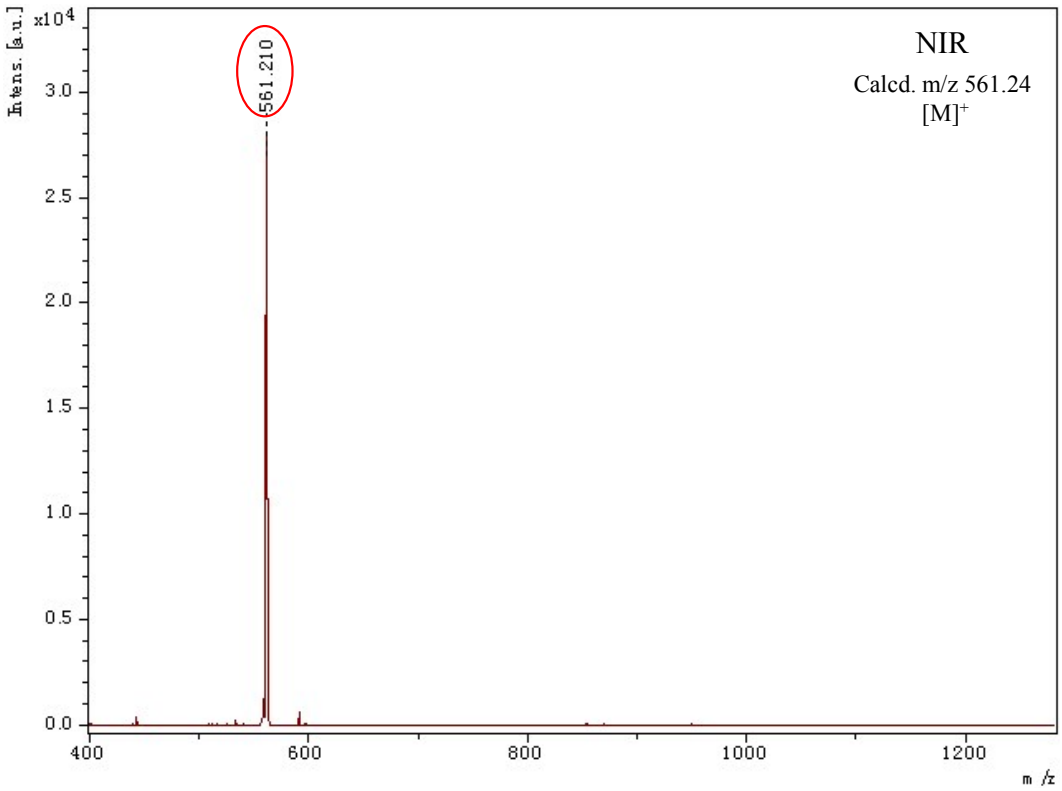

Fig. S3. Mass spectra of compound NIR.

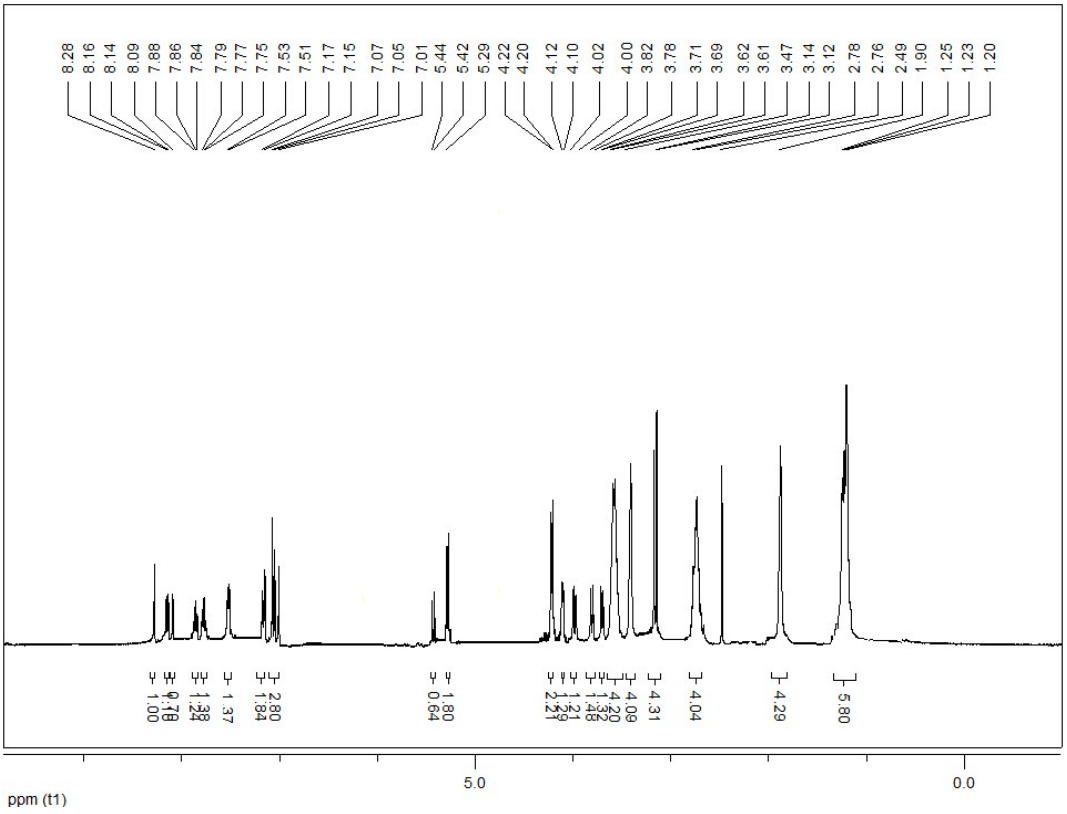

Fig. S4. ^{1}H NMR spectra of compound Gal-NIR in DMSO-d_6.

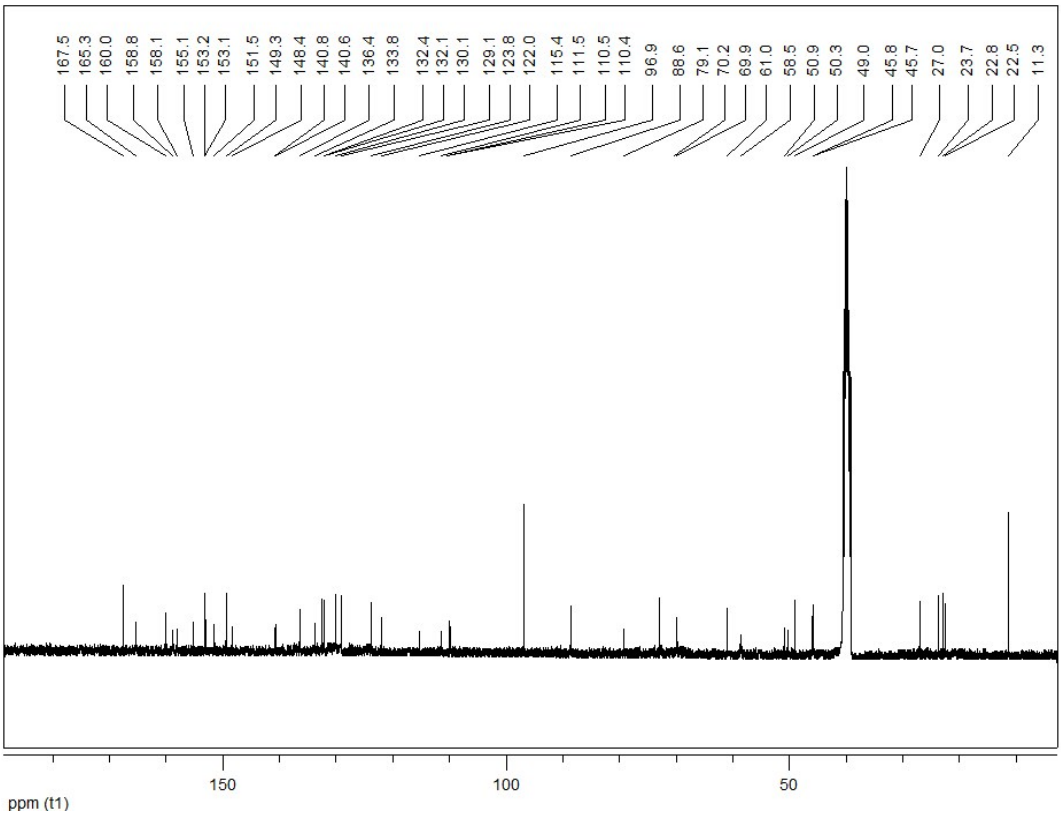

Fig. S5. ^{13}C NMR spectra of compound Gal-NIR in DMSO-d_6.

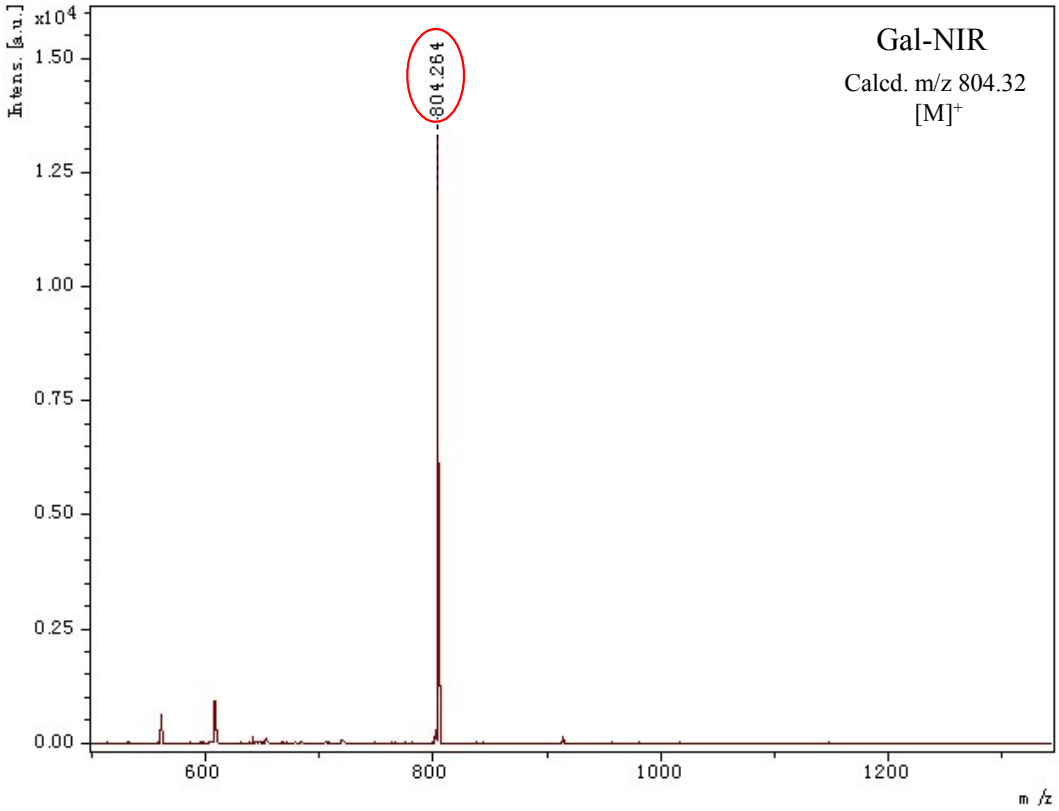

Fig. S6. Mass spectra of compound Gal-NIR.

3. Spectral data.

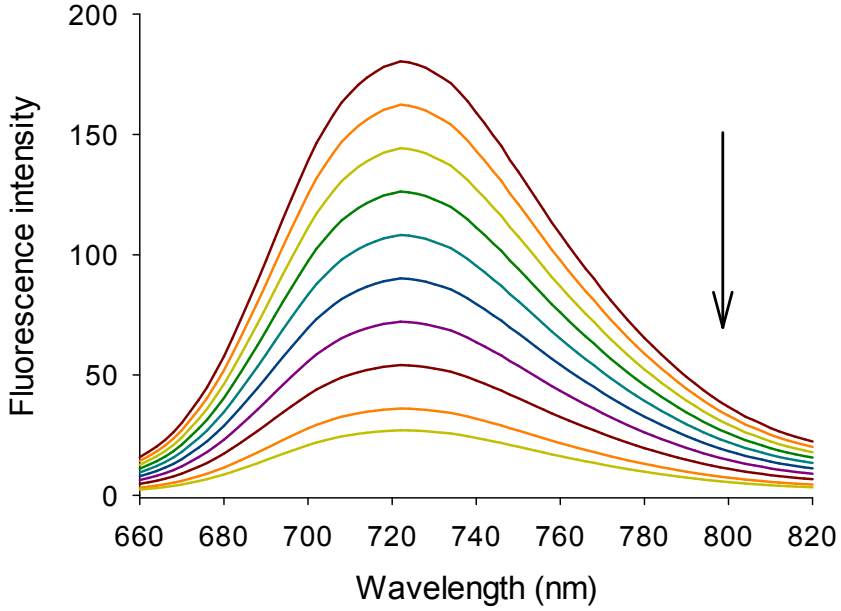

Fig. S7. Fluorescence spectra of Gal-NIR (5 μM) upon adding various amounts of $ONOO^-$ (0, 0.5, 1.0, 2.0, 3.0, 5.0, 7.0, 10.0, 13.0, 15.0 μM) in PBS buffer solution (pH 7.4). λ_{ex} = 650 nm.

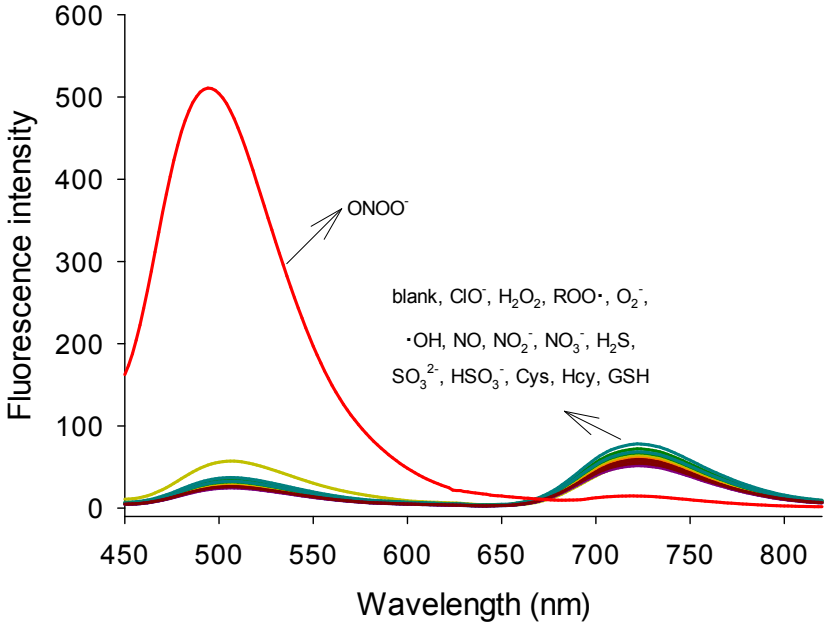

Fig. S8. The fluorescence spectra of Gal-NIR (5 μM) to $ONOO^-$ (15 μM) and other various species (150 μM) in PBS buffer solution (pH 7.4). λ_{ex} = 440 nm.

The effect of pH on the fluorescence intensity ratio (F_{500}/F_{720}) before and after the addition of $ONOO^-$ was tested (Fig. S9). Gal-NIR possesses a good ratiometric fluorescence response toward $ONOO^-$ in pH range 7.0-8.0. The results show that the probe can be applied at the physiological condition (pH 7.4). Also, the time-dependent fluorescence intensity changes of Gal-NIR in the presence of $ONOO^-$ were studied (Fig. S10). The ratio (F_{500}/F_{720}) promptly increases upon the addition of 15 μM $ONOO^-$ and reaches a plateau almost within 10 min, suggesting that Gal-NIR could serve as a fast-response probe for $ONOO^-$. Moreover, almost no detectable signal change is observed over 6 h, indicating that Gal-NIR is stable (Fig. S11).

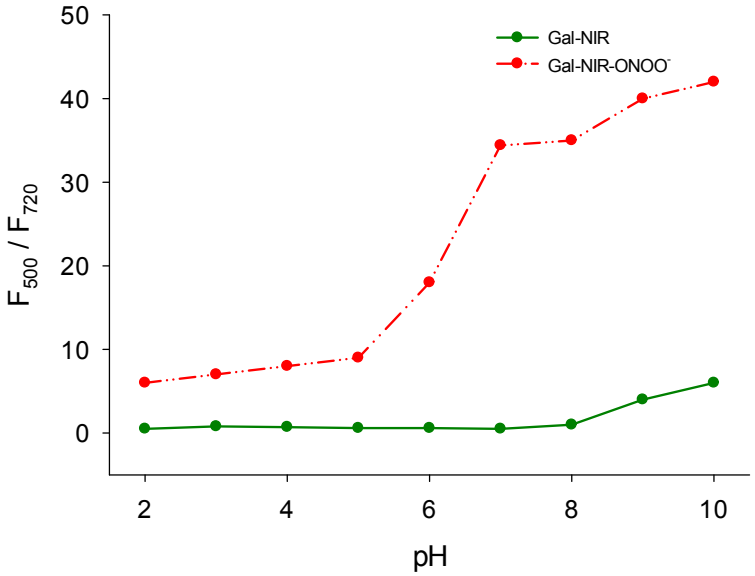

Fig. S9. Effect of pH on the fluorescence intensity ratio (F_{500}/F_{720}) of Gal-NIR (5 μM) before and after the addition of $ONOO^-$ (15 μM). λ_{ex} = 440 nm.

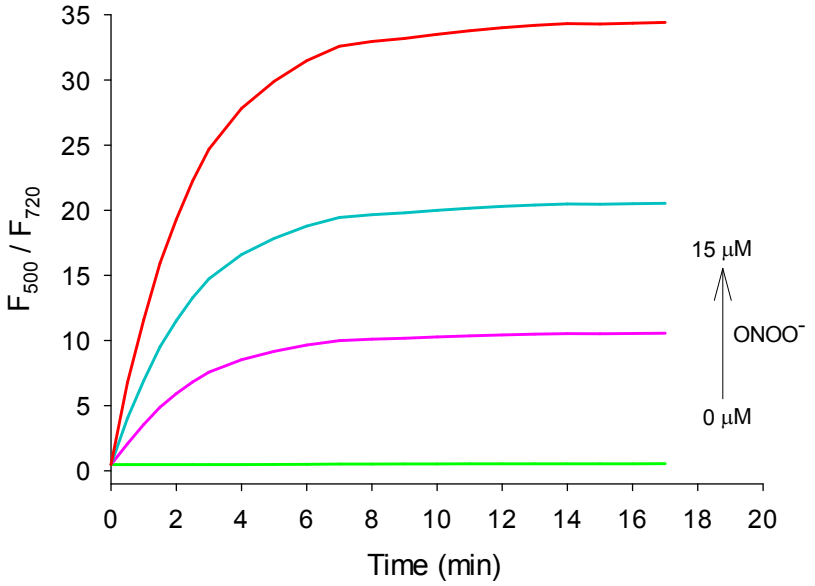

Fig. S10. Time-dependent fluorescence intensity ratio (F_{500}/F_{720}) of Gal-NIR (5 μM) to $ONOO^-$ (0, 1.0, 5.0, 10, 15 μM) in PBS buffer solution (pH 7.4). λ_{ex} = 440 nm.

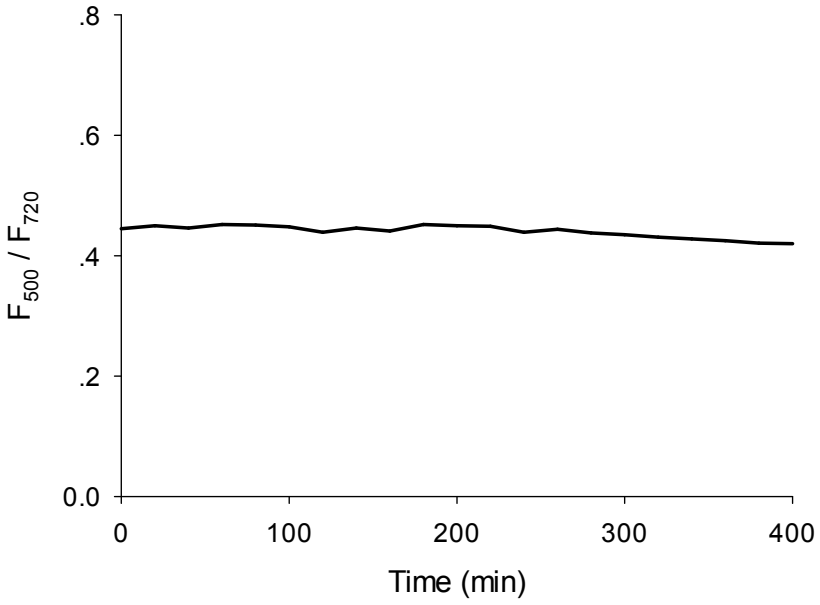

Fig. S11. Time-dependent fluorescence intensity ratio (F_{500}/F_{720}) of Gal-NIR (5 μM) in PBS buffer solution (pH 7.4). λ_{ex} = 440 nm.

4. Response mechanism.

Based on the evidence from the change of fluorescence spectra, a possible response mechanism of Gal-NIR to $ONOO^-$ was proposed (Fig. S12). Gal-NIR displays NIR emission due to the large π-conjugation system. After adding $ONOO^-$, the oxonium group of the probe suffers from nucleophilic reaction between $ONOO^-$ with ketone and then oxidative cleavage to finally yield a carboxylic acid product (coumarin 343), which gives a green fluorescence owing to its small π-conjugation system. So, the probe exhibits a ratiometric fluorescence response towards $ONOO^-$ with large emission shift. In order to prove the response mechanism of Gal-NIR to $ONOO^-$, the absorption and fluorescence spectra were studied (Fig. S13). After adding $ONOO^-$, Gal-NIR displays increased absorption at 440 nm, which is similar to that of coumarin 343. Similarly, when reacted with $ONOO^-$, Gal-NIR exhibits an enhanced emission at 500 nm, which is essentially identical with the emission of coumarin 343. HPLC experiment was also carried out to illustrate the proposed reaction mechanism (Fig. S14). Gal-NIR itself displays a signal peak at 2.51 min. Upon adding $ONOO^-$, the signal for Gal-NIR disappears and one new signal at 3.38 min (the similar retention time with coumarin 343) appears. Most importantly, the mass spectra analysis was performed to confirm the proposed mechanism (Fig. S6 and Fig. S15). For free Gal-NIR, the peak is at m/z = 804.3. After the treatment of $ONOO^-$, a new peak at m/z = 308.1 corresponding to coumarin 343 arises. All the results prove that Gal-NIR can be cleaved efficiently by $ONOO^-$ and transforms into coumarin 343, which is in good agreement with the proposed mechanism.

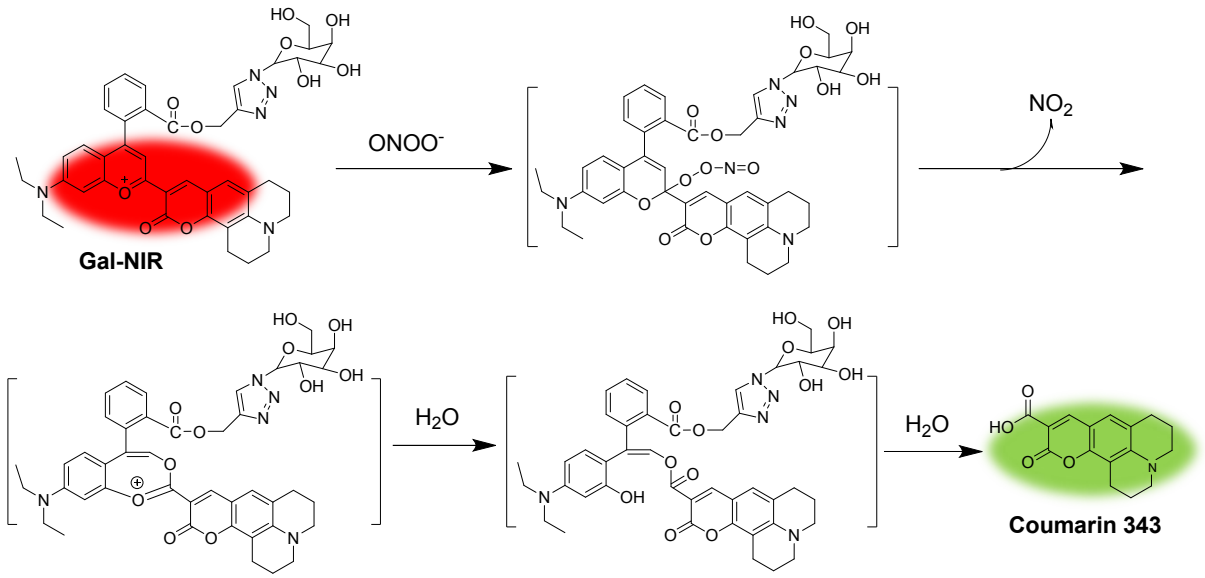

Fig. S12. Proposed reaction mechanism for Gal-NIR and $ONOO^-$.

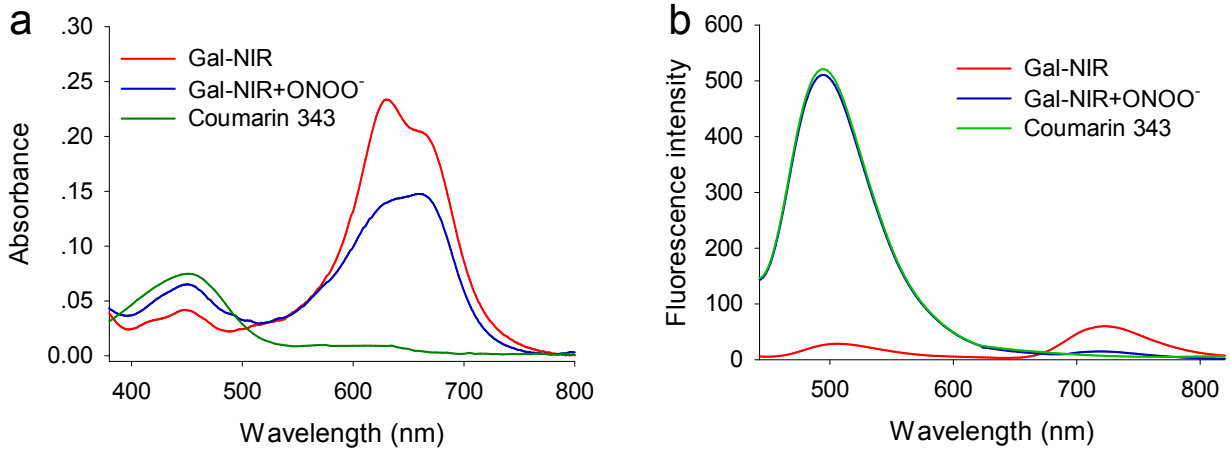

Fig. S13. (a) Absorption spectra of coumarin 343 (5 μM), and Gal-NIR (5 μM) before and after the addition of $ONOO^-$ (15 μM) in PBS buffer solution (pH 7.4). (b) Fluorescence spectra of coumarin 343 (5 μM), and Gal-NIR (5 μM) before and after the addition of $ONOO^-$ (15 μM) in PBS buffer solution (pH 7.4). λ_{ex} = 440 nm.

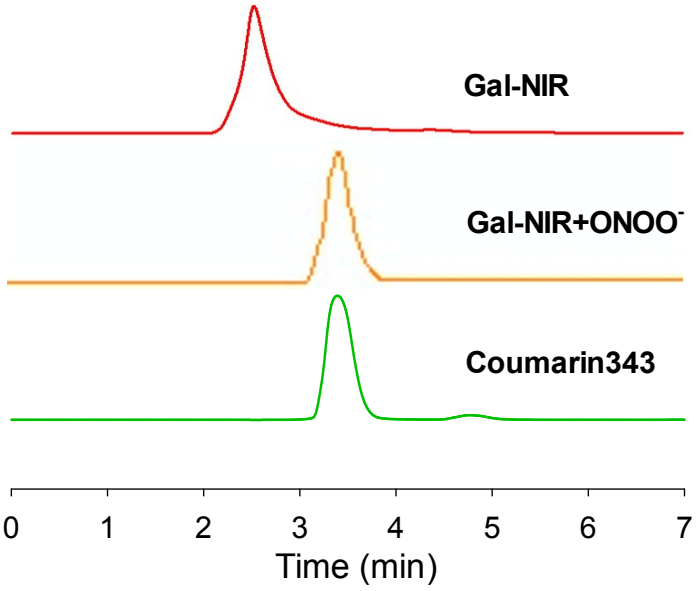

Fig. S14. HPLC chromatograms of Gal-NIR before and after the addition of $ONOO^-$. The HPLC mobile phase: solvent A (CH_3OH), solvent B (water), A/B = 4/1 (v/v).

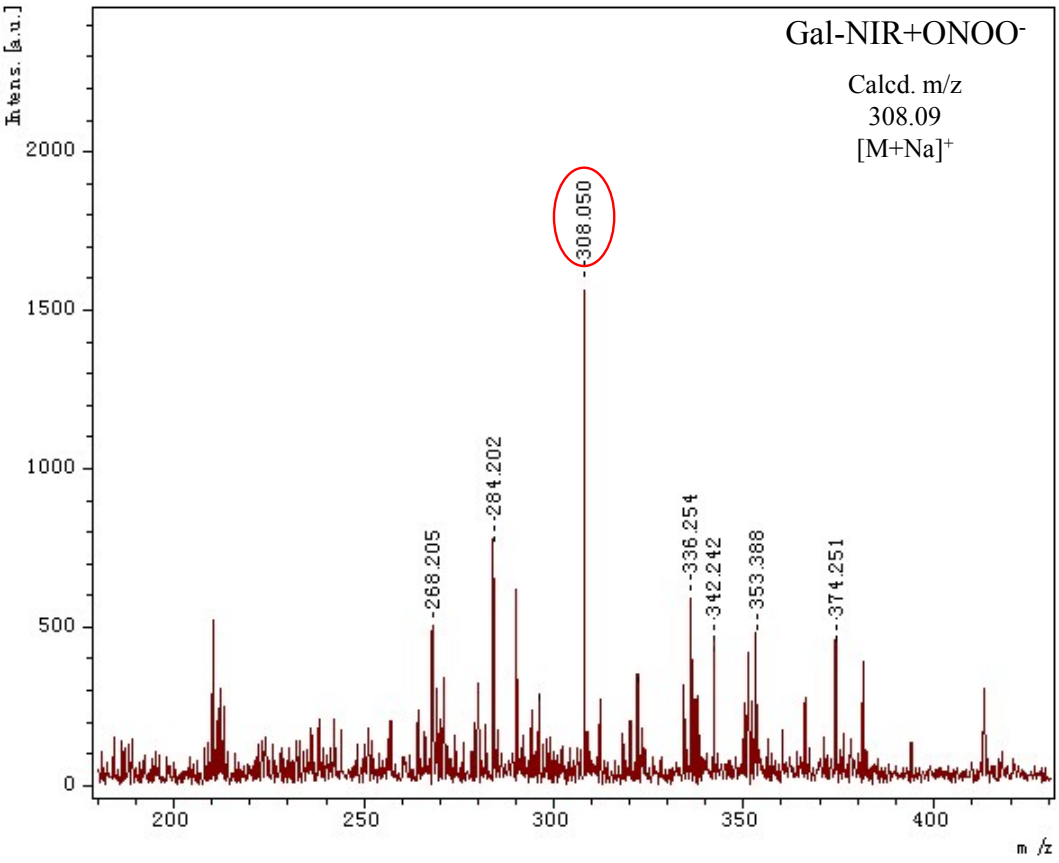

Fig. S15. Mass spectra of Gal-NIR with $ONOO^-$.

5. Biological assays.

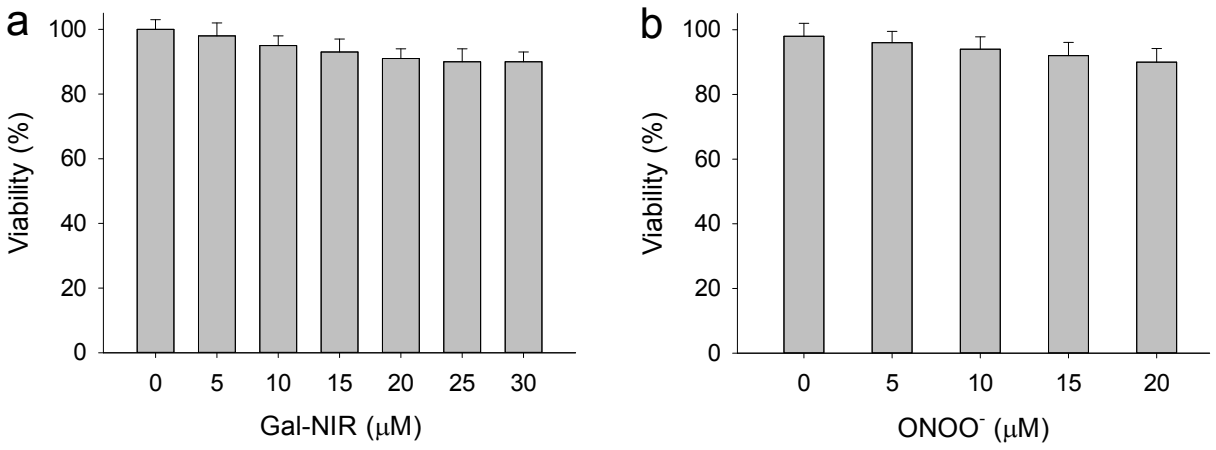

Fig. S16. MTT assay for estimating cell viability (%). (a) HepG2 cells were treated with various concentrations of Gal-NIR (0-30 μM). (b) HepG2 cells were treated with Gal-NIR (5 μM) and various concentrations of $ONOO^-$ (0-20 μM).

The probe was used for detecting exogenous and endogenous $ONOO^-$ in HepG2 Cells (Fig. S17). When the cells are treated with Gal-NIR alone, very weak fluorescence in green channel and strong fluorescence in red channel are observed (Fig. S17a). 3-Morpholinosydnonimine (SIN-1) was employed as exogenous source of $ONOO^-$. When the cells are treated with SIN-1 and Gal-NIR, a dramatic fluorescence quenching in red channel and a remarkable fluorescence enhancement in green channel are seen (Fig. S17b). Moreover, the fluorescence intensity ratio (F_{green}/F_{red}) enhances with time and arrives at the maximum (5.5-fold) after 30 min (Fig. S18). Lipopolysaccharide (LPS) are known to generate endogenous $ONOO^-$. After the incubation with LPS, the ratio (F_{green}/F_{red}) shows 5.1-fold enhancement (Fig. S17c). However, the increase of ratio (F_{green}/F_{red}) caused by LPS is reduced significantly by Cys (an important antioxidant defender, Fig. S17d). All these experimental results suggest that probe Gal-NIR can monitor exogenous and endogenous $ONOO^-$ level in cells by fluorescence imaging. For living cells, $ONOO^-$ is mainly produced in mitochondria, so the co-localization experiments was done to study whether Gal-NIR can target mitochondria (Fig. S19). The red channel fluorescence of Gal-NIR shows excellent overlay with green channel fluorescence of Mito-Tracker Green, with high Pearson's colocalization coefficient (0.96), indicating that Gal-NIR can specifically target the mitochondria of the living cells.

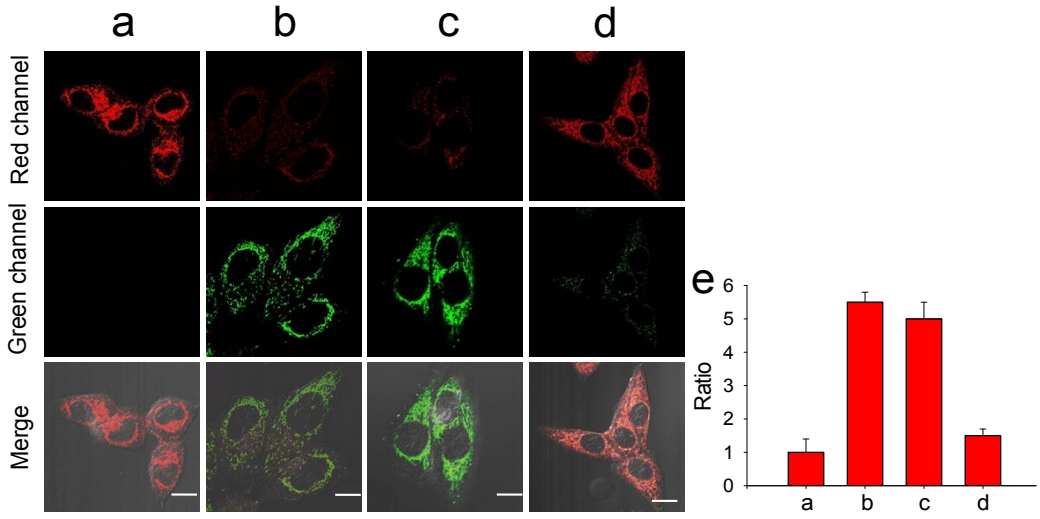

Fig. S17. Fluorescence image for $ONOO^-$ in HepG2 cells. (a) The cells were treated with Gal-NIR (5 μM) for 30 min. (b) The cells were pretreated with SIN-1 (100 μM) for 30 min, and then incubated with Gal-NIR (5 μM) for 30 min. (c) The cells were pretreated with LPS (1 mg/mL) for 10 h and then incubated with Gal-NIR (5 μM) for 30 min. (d) The cells were pretreated with Cys (200 μM) for 30 min, followed by treating with LPS (1 mg/mL) for 10 h and then stained with Gal-NIR (5 μM) for 30 min. (e) Fluorescence intensity ratio (F_{green}/F_{red}) is obtained from image a-c and the ratio of image a is defined as 1.0. Scale bar: 10 μm. Red channel: λ_{ex} = 635 nm, λ_{em} = 650-750 nm; Green channel: λ_{ex} = 488 nm, λ_{em} = 500-550 nm.

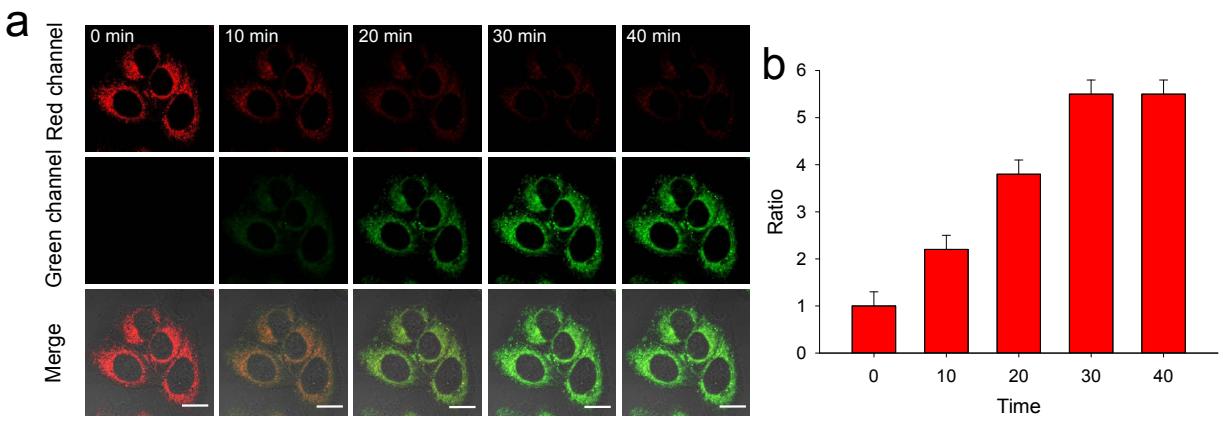

Fig. S18. The time-dependent fluorescence responses to exogenous $ONOO^-$ in HepG2 cells. (a) The cells were treated with SIN-1 (100 μM) for 30 min, and then incubated with Gal-NIR (5 μM) at different time points: 0 min, 10 min, 20 min, 30 min, 40 min. (b) The ratio of fluorescence intensity (F_{green}/F_{red}) is obtained from a and the ratio at 0 min is defined as 1.0. Scale bar: 10 μm. Red channel: λ_{ex} = 635 nm, λ_{em} = 650-750 nm; Green channel: λ_{ex} = 488 nm, λ_{em} = 500-550 nm.

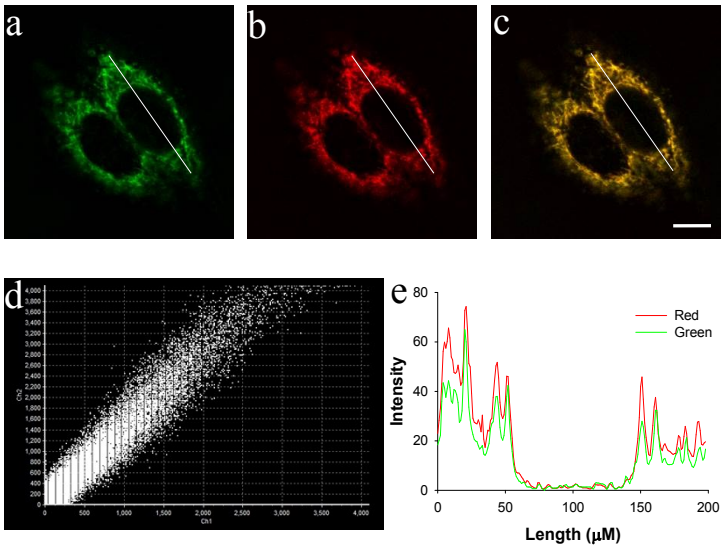

Fig. S19. Co-localization imaging of HepG2 cells staining with Gal-NIR and Mito-Tracker Green. (a) The cells were stained with Mito-Tracker Green (1 μM) for 30 min on green channel (λ_{ex} = 488 nm, λ_{em} = 500-550 nm). (b) The cells were stained with Gal-NIR (5 μM) for 30 min on red channel (λ_{ex} = 635 nm, λ_{em} = 650-750 nm). (c) Merged image of images a and b. (d) Intensity scatter plot. (e) The intensity profile of linear regions of interest (ROI) across the cells. Scale bar: 10 μm.

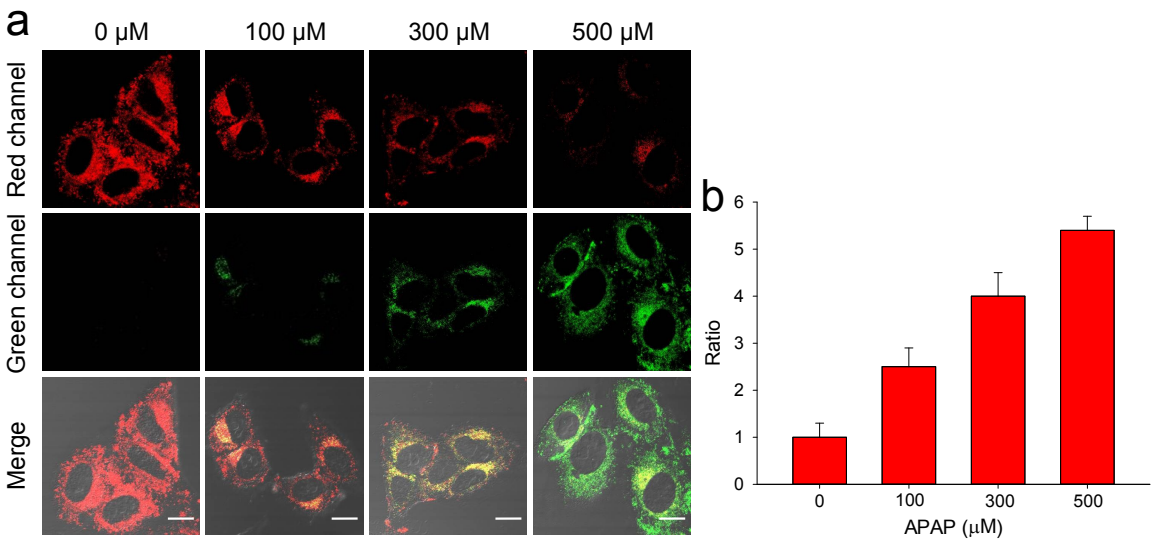

Fig. S20. (a) Fluorescence images of HepG2 cells incubated with different concentrations of APAP (0, 100, 300, 500 μM) for 12 h, and then stained with Gal-NIR (5 μM) for 30 min. (b) The ratio of fluorescence intensity (F_{green}/F_{red}) is obtained from a and the ratio at 0 μM is defined as 1.0. Scale bar: 10 μm. Red channel: λ_{ex} = 635 nm, λ_{em} = 650-750 nm; Green channel: λ_{ex} = 488 nm, λ_{em} = 500-550 nm.

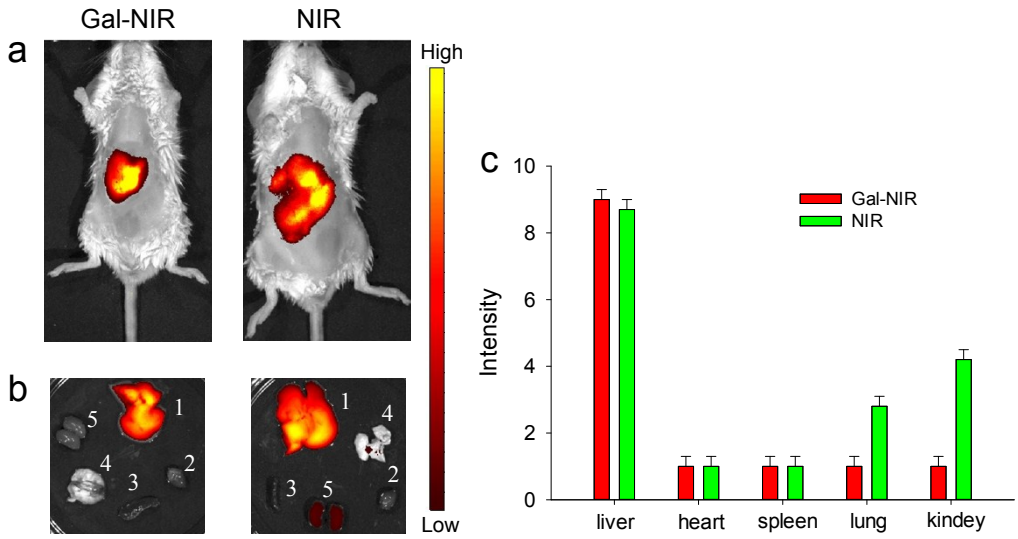

Fig. S21. (a) Fluorescence imaging of Gal-NIR (100 μL, 200 μM) or NIR (100 μL, 200 μM) in BALB/c mice. (b) Fluorescence imaging of Gal-NIR and NIR in the main organs. 1: liver, 2: heart, 3: spleen, 4: lung, 5: kindey. (c) Relative fluorescence intensity in b and the lowest fluorescence intensity is defined as 1.0. The mice imaging were operated only in red channel: λ_{ex} = 640 nm; λ_{em} = 680-780 nm.